

Final Draft
of the original manuscript:

Handge, U.A.; Wolff, M.F.H.; Abetz, V.; Heinrich, S.:
**Viscoelastic and dielectric properties of composites of
poly(vinyl butyral) and alumina particles with a high
filling degree**
In: Polymer (2015) Elsevier

DOI: [10.1016/j.polymer.2015.11.047](https://doi.org/10.1016/j.polymer.2015.11.047)

Viscoelastic and dielectric properties of composites of poly(vinyl butyral) and alumina particles with a high filling degree

Ulrich A. Handge,^{1,*} Michael F.H. Wolff,² Volker Abetz^{1,3} and Stefan Heinrich²

¹*Institute of Polymer Research, Helmholtz-Zentrum Geesthacht, Max-Planck-Strasse
1, 21502 Geesthacht, Germany*

²*Institute of Solids Process Engineering and Particle Technology, Hamburg
University of Technology, Denickestrasse 15, 21073 Hamburg, Germany*

³*Institute of Physical Chemistry, University of Hamburg, Grindelallee 117, 20146
Hamburg, Germany*

Abstract

Filler-filler and filler-matrix interactions in polymer composites increase with filler concentration and strongly influence the mechanical and rheological properties of polymer composites. By means of the spouted bed spray granulation process polymer composites with an extremely high concentration of inorganic fillers can be prepared. In this work, the viscoelastic properties of highly filled composites of poly(vinyl butyral) (PVB) and alumina particles are studied in the glassy, entanglement and terminal flow regime of poly(vinyl butyral). Ceramic-polymer composites with a volume concentration of inorganic particles between 61 vol% and 77 vol% were prepared. Such large filler fractions imply a strong effect of filler-filler interactions on the viscoelastic properties of the composite. Dynamic-mechanical thermal analysis reveals that the composites are characterized by a predominantly elastic behaviour below and above the glass transition temperature of the polymer phase because of strongly pronounced filler-filler and polymer-filler interactions. A phenomenological equation is proposed in order to describe the reinforcement effect which implies an increase of storage modulus by a factor of up to four orders of magnitude. The results of frequency and strain sweeps in the oscillatory mode show that the polymer phase strongly influences the deformation of the contact network of inorganic particles. Differential scanning calorimetry and broadband dielectric spectroscopy indicate that the glass transition temperature of poly(vinyl butyral) does not significantly differ within experimental resolution for pristine PVB and the PVB phase in the composites.

Keywords: Polymer composites; Spouted bed spray granulation; Dynamic-mechanical thermal analysis; Broadband dielectric spectroscopy; Filler networks

*Corresponding author (ulrich.handge@hzg.de)

1. Introduction

The preparation of ceramic-polymer composites opens an attractive route for combining large values of ductility and strength in a single material. In addition to the properties of the pristine components, the microstructure of hybrid materials influences their macroscopic properties [1]. During the last decades, several techniques were developed for preparation of ceramic-polymer composites, e.g., for the development of hierarchically structured materials [2, 3]. In order to achieve optimum mechanical properties such as tensile modulus and hardness, a large fraction of inorganic phase in the ceramic-polymer composite is desired. Very large volume fractions generally lead to morphologies which differ from the matrix morphology at low filler concentrations. At high volume fractions, a network which consists of fillers being, at least partially, in contact is formed. This so-called contact network (percolation network) and hence the viscoelastic properties of the composite are strongly influenced by filler-filler and polymer-filler interactions. In addition to enhancement of mechanical properties, highly filled polymer composites can be also prepared in order to achieve tailored thermal or magnetic functions [4-6]. Recently, the spouted bed spray granulation process and subsequent hot-pressing was applied for the preparation of ceramic-polymer composites [7]. Composites with a volume fraction of ceramic particles up to 78 vol% and a porosity lower than 2 vol% were prepared. In their work, Wolff et al. discussed possible failure modes in the composites under loading. Because of their enhanced insulating properties, the dielectric properties of highly filled ceramic-polymer composites are also of interest. The investigations of Brandt et al. [8] at test temperatures below the glass transition of the poly(methyl methacrylate) component revealed a strong influence of the ceramic component on the dielectric properties of the composite.

Generally, the pronounced temperature dependence of the viscoelastic properties of polymers yields a mechanical response of ceramic-polymer composites which is very sensitive to temperature changes. Consequently, a strong need exists in order to study the temperature dependence of the mechanical properties of highly filled polymer composites. Such results give valuable insight into the viscoelastic properties of materials with a microstructure inspired by nature, since the combination of the spouted bed spray granulation process and subsequent hot-pressing is a base for preparation of multi-level hierarchical composites [9].

The mechanical and flow properties of filled composites are strongly influenced by interparticle and polymer-filler interactions [10, 11]. Particle-matrix and filler-filler interactions in polymer composites were investigated in several theoretically and experimentally oriented publications [12-19]. The reinforcement caused by solid fillers at dilute concentrations can be described by the theories of Guth and Gold [20, 21]

and Smallwood [22]. Aranguren et al. [23] discussed the influence of molar mass of the polymer component on the rheological properties of polymers filled with unmodified and modified silica particles. Filler agglomerates are broken up above a critical strain amplitude. Furthermore, the functionalization of the surface of the silica particles strongly influences the dynamic moduli of the composite. In the work of Bigg [24], the rheological properties of composites of a low density polyethylene (LDPE) and alumina particles were studied. In their work, the composites were prepared by a conventional mixing process leading to a volume fraction of the ceramic particles of 57%. The influence of strain amplitude on the rheological properties in the melt state was elucidated. Increasing the volume fraction of fillers leads to a strong increase of viscosity which is disadvantageous for extrusion. Experiments below the melting temperature of LDPE were not performed in the work of Bigg. In the work of Saini et al. [25] several highly filled ferrite-polymer composites were prepared, and the influence of particle concentration and temperature was analyzed in the melt state. In the review article of Cassagnau, the linear viscoelastic properties of suspensions and polymer melts filled with nanoparticles are summarized [26]. In this article, the interplay of viscous forces, orientation effects and breakup/aggregation phenomena are discussed.

In a series of theoretical studies, equations for the prediction of mechanical moduli of filled polymers were derived, see, e.g., the works of Halpin and Kardos [27, 28]. For low filling degrees, the polymer matrix mainly determines the mechanical and rheological response. Thermoplastic polymers behave like a physically crosslinked (i.e. temporary) polymer network in the so-called rubbery regime. Consequently, a similar behavior exists for physically and chemically (i.e. elastomers) crosslinked polymers. The strength of interaction of the polymer chains with the fillers is of high importance, which is demonstrated, e.g., by the Payne effect [29]. Filler-filler (formation and breakup of a filler network) and polymer-filler (partial immobilization of polymer chains) interactions lead to the Payne effect which was the topic of a series of research studies, see the works of Heinrich and Klüppel [30] and Klüppel [31] for a review. In elastomers which are filled with carbon black, time-dependent aggregation appears. Several models were developed in order to describe this effect [32]. The attractive forces between adjacent nanofillers depend on the type of fillers and are strongly pronounced in the case of carbon black or silica fillers [33]. Dielectric studies of electrically conductive composites with carbon black fillers were performed in order to analyze the fractal filler network. The experimental data of Kummali et al. [34] using so-called nano-dielectric spectroscopy do not give any indication of an immobilized polymer layer around silica nanoparticles in styrene-butadiene-rubber (SBR). The influence of water on the Maxwell-Wagner-Sillars polarization in silica-filled styrene-butadiene rubber compounds was investigated by Otegui et al. [35]. A

larger water content is associated with a shift of the relaxation peak to higher frequencies.

Previous studies mainly focused on a limited temperature interval and to significantly lower volume fractions of the filler particles than can be achieved by the spouted bed spray granulation process. The application of the spouted bed spray granulation process and subsequent hot-pressing allows the preparation of ceramic-polymer composites with an extremely high filler concentration [7]. In this work, the viscoelastic properties of highly filled composites of poly(vinyl butyral) (PVB) and alumina particles (α -Al₂O₃) are investigated. We focus on the temperature dependence of the dynamic moduli and study the influence of particle size and concentration. The objective of this study is to analyze the influence of viscoelasticity of the polymer phase on the properties of the composite which is characterized by a contact network of particles. As a first approach, an amorphous thermoplastic polymer was chosen as polymeric component. Because of the strong temperature dependence of the viscoelastic properties of amorphous homopolymers, amorphous thermoplastic polymers are ideally suited to study the influence of the polymeric component in detail.

2. Experimental

2.1. Materials

The available spouted bed spray granulation apparatus requires a polymer which is soluble in a non-hazardous solvent. Therefore poly(vinyl butyral) (which can be dissolved in ethanol) was chosen as polymer component and kindly provided by Kuraray Specialities Europe GmbH (Frankfurt am Main, Germany). Poly(vinyl butyral) is an amorphous thermoplastic polymer and synthesized in a reaction of aqueous poly(vinyl alcohol) solution with butyraldehyde in the presence of small amounts of mineral acid. This reaction leads to a block copolymer of vinylalcohol (18-21 wt%) and butyraldehyde with an additional small fraction of vinyl acetate units (1-4 wt%) [36]. The molecular weight of poly(vinyl butyral) was determined by gel permeation chromatography (GPC) using polystyrene as standard. The GPC measurements were carried out in dimethylacetamide on a Waters instrument (Waters GmbH, Eschborn, Germany) with polystyrene gel columns (porosities of 10, 10², 10³, 10⁴ and 10⁵ Å) and UV and RI detectors. The results of molecular characterization are shown in Table 1.

In order to prepare highly filled polymer composites, alumina (α -Al₂O₃) particles with different particle size distributions were used in our investigations. Alumina was chosen because it is a good model material for a hard, non-hazardous ceramic with a

large abundance in nature and with a good adhesion to poly(vinyl butyral). Depending on the degree of filling, either one coarse fraction or two fractions (a coarse one and a fine one with a weight ratio of 60/40) of alumina were used. Monodisperse particle size distributions would be optimum for comparison of experimental data with theoretical results, but were not accessible. Polydisperse particle size distributions appear in technological applications. The coarse particle fraction was fused alumina F360 (Kuhmichel Abrasiv GmbH, Ratingen, Germany) with a nominal median (volume size distribution) $d_{50,3}$ of $d_{50,3} = 26.3 \mu\text{m}$ or alumina (Pieplow & Brandt GmbH, Henstedt-Ulzburg, Germany) with a median of the volume size distribution of $d_{50,3} = 14.5 \mu\text{m}$, $18.2 \mu\text{m}$ and $44.0 \mu\text{m}$, respectively. The fine particle fraction was either alumina with a median of $d_{50,3} = 5.5 \mu\text{m}$ (Pieplow & Brandt GmbH) or alumina CT 3000 SG from Almatris Inc. ($d_{50,3} \approx 0.5 \mu\text{m}$). The density of the alumina particles is approximately 3.98 g/cm^3 . The median $d_{50,3}$ of the particle volume size distribution of the fluidized particle size fractions was determined with the Camsizer XT (Retsch Technology GmbH, Haan, Germany) and with a particle size analyzer LS13320 (Beckman Coulter Inc., Brea (CA), USA) using the technique of static light scattering for the powder with a particle median smaller than $1 \mu\text{m}$. The composites are summarized in Table 2.

2.2. Thermal analysis

In order to determine the glass transition temperature T_g of the PVB phase, differential scanning calorimetry (DSC) measurements were carried out in a nitrogen atmosphere. A calorimeter DSC 1 (Mettler-Toledo, Gießen, Germany) was used for the investigations. Before the experiment, the powder was dried under vacuum at $40 \text{ }^\circ\text{C}$ for several days. Then approximately 9 mg of polymer were placed in a $40 \mu\text{L}$ aluminum pan with a mono-perforated lid. A heating-cooling-heating cycle (temperature interval $25 \text{ }^\circ\text{C}$ to $200 \text{ }^\circ\text{C}$) was applied. Several runs with several new samples using different heating rates in the second heating interval were performed. The value of T_g was determined using the data of the second heating cycle (midpoint method DIN 51007, heating rate 1 K/min). In order to compare the DSC data of the pristine polymer with data of the composite, DSC experiments with the composite Al_2O_3 -PVB 70.9 were also performed. The sample weight for the composite was approximately 20 mg .

Thermal gravimetric analysis (TGA) of PVB and the composite Al_2O_3 -PVB 70.9 was carried out using a TG 209 F1 Iris instrument (Netzsch, Selb, Germany) in an argon atmosphere. The temperature range was $25 \text{ }^\circ\text{C}$ to $1100 \text{ }^\circ\text{C}$. The heating rate was 10 K/min .

2.3. Spouted bed spray granulation process

A spouted bed spray granulation process was applied to prepare the ceramic-polymer granules which were then further processed via hot-pressing. The coarse (median larger than 10 μm) alumina particle size fraction was fluidized in a spouted bed apparatus as shown schematically in Fig. 1. Ambient air at a temperature of 40 $^{\circ}\text{C}$ in the fluidizing zone was chosen as process gas. The spraying liquid consisted of poly(vinyl butyral) dissolved in ethanol. For reaching the highest filling degrees, fine alumina particles (median $d_{50,3} \approx 0.5 \mu\text{m}$ and $d_{50,3} \approx 5.5 \mu\text{m}$, respectively) were additionally suspended in the spraying liquid. During the granulation process the spraying liquid was sprayed onto the fluidized particles with a spraying rate (mass of spraying liquid per unit time which was injected into the process chamber during the granulation process) of several g/min. The experimental parameters were optimized in order to avoid overspraying. Then the coated particles were hot-pressed using an automatic press PWV 300 (Paul-Otto Weber GmbH, Remshalden, Germany) for 60 min at a temperature of 160 $^{\circ}\text{C}$ and a pressure of 750 MPa. A diamond saw (Brillant 200, ATM GmbH, Mammelzen, Germany) was used for cutting specimens with rectangular cross sections. The prepared specimens are listed in Table 2. In this study, filling degree and particle size were varied in order to study the influence of these parameters on the properties of the ceramic-polymer composites. The volume fractions were chosen in order to achieve four distinctly different filling degrees. Details on the spray granulation process and the hot-pressing can be found in Wolff et al. (2014). Reference samples of pristine poly(vinyl butyral) were prepared by hot-pressing powder of PVB at 160 $^{\circ}\text{C}$ for 60 min at a reduced pressure.

2.4. Water content measurements

In order to determine qualitatively the maximum water uptake of poly(vinyl butyral), cylindrical samples with a diameter of 24 mm and a thickness of 2 mm were dried at 40 $^{\circ}\text{C}$ under vacuum for a period of at least 4 days. Then the samples were placed in ambient air and room temperature and the relative water uptake was determined. The stationary value of water uptake was attained after 14 days and was equal to $1.25 \pm 0.01 \text{ wt}\%$. For rheological testing, samples (pristine poly(vinyl butyral) and the composites) were stored at 40 $^{\circ}\text{C}$ under vacuum for several days. The daily weighing of the samples revealed that the samples did not change their mass after a couple of days. The mass loss (which is presumed to be the result of water loss) was in the order of 0.9 - 1.0 wt% for pristine poly(vinyl butyral) and 0.1 - 0.2 wt% for the composites. These data confirm that the water uptake in the composite is caused by the PVB component.

2.5. Rheological experiments and dynamic-mechanical thermal analysis

The samples prepared by the spouted bed spray granulation process and subsequent hot-pressing were used for dynamic-mechanical thermal analysis (DMTA). The samples had rectangular cross-sections with dimensions of approximately $2 \times 5 \text{ mm}^2$. The length of the samples was in the order of 35 to 40 mm. Experiments in the torsion mode were performed using the rotational rheometer ARES (Rheometric Scientific Inc., Piscataway (NJ), USA). A nitrogen atmosphere was applied. The frequency was set to $f = 1 \text{ Hz}$. Before the experiments, a strain sweep at a temperature of $25 \text{ }^\circ\text{C}$ in the interval of 0.02% to 0.2% was carried out in order to determine the linear viscoelastic range. In the subsequent temperature sweep, the strain amplitude was set to $\gamma_0 = 0.05\%$. The temperature range in this test mode was $25 - 150 \text{ }^\circ\text{C}$, and the heating rate was 1 K/min . The sequence for testing the samples was chosen arbitrarily. Furthermore, isothermal strain and frequency sweeps were also carried out at selected temperatures (30, 45, 53, 60, 68, 90 and $120 \text{ }^\circ\text{C}$). The strain amplitude in the strain sweeps ranged from 0.02 to 0.2%. In the frequency sweeps, the frequency range was $\omega = 0.01 - 100 \text{ rad/s}$ starting at the highest frequency. The strain amplitude was $\gamma_0 = 0.05\%$. The time for temperature equilibration was 15 min.

Powder of poly(vinyl butyral) was dried under vacuum for a couple of days at a temperature of $40 \text{ }^\circ\text{C}$. Cylindrical samples of poly(vinyl butyral) were prepared by compression-moulding at $110 \text{ }^\circ\text{C}$ for a period of 4 min with a compressive force of 50 kN. Then frequency sweeps (range of angular frequency between 0.01 and 100 rad/s with a strain amplitude of $\gamma_0 = 1\%$) at temperatures of 75, 90, 120 and $150 \text{ }^\circ\text{C}$ were carried out using a rotational rheometer MCR 502 (Anton Paar GmbH, Graz, Austria) in a nitrogen atmosphere. The frequency sweeps were performed in the range from high to low frequencies. Furthermore, DMTA experiments with a plate-plate geometry (plate diameter 8 mm, gap 2 mm) at a frequency of $f = 1 \text{ Hz}$ and a strain amplitude of $\gamma_0 = 1\%$ in the range from $150 \text{ }^\circ\text{C}$ to $50 \text{ }^\circ\text{C}$ were also carried out.

2.6. Broadband dielectric spectroscopy

The dielectric properties of pristine poly(vinyl butyral) and of the composite Al_2O_3 -PVB 70.9 were characterized by dielectric spectroscopic measurements. An Alpha-AN high resolution dielectric analyzer (Novocontrol Technologies GmbH, Montabaur, Germany) was used for the investigations. The samples (see Section 2.3. for sample preparation) were placed between two cylindrical brass electrodes with a diameter of 40 mm. The contribution of the air to the measured capacity was corrected in order to determine the pure response of the sample. Similar to the rheological experiments, isothermal measurements in the frequency range from 10^7 Hz to 10^{-2} Hz in the

temperature range of 30 °C to 80 °C were performed in order to investigate the temperature range of glass transition. Furthermore a temperature ramp in the interval from 30 °C to 150 °C in increments of 2 °C at a frequency of 100 Hz was also carried out. The applied voltage was 2 V in all experiments.

2.7. Scanning electron microscopy

Scanning electron microscopy investigations (SEM) were carried out in order to analyse the microstructure of the composites. The sample was notched and then broken under liquid nitrogen. Then the fracture surface was sputtered with a carbon layer (thickness of approximately 4 nm) using an argon ion beam system (PECS II, Gatan Inc., Pleasanton (CA), USA). Scanning electron microscopes of type Merlin and of type LEO 1530 Gemini (Zeiss, Oberkochen, Germany) equipped with a field emission cathode were used for the investigation. The voltage was varied and ranged between 4 and 10 kV. A secondary electron detector (Fig. 2), a back scattering (Figs. 3(a) and (b)) and a primary electron detector (Fig. 3(c)) were used for the investigations.

3. Results and discussion

Figure 2 presents a scanning electron micrograph of the alumina particles (Kuhmichel Abrasiv GmbH). The particles have an irregular shape with sharp edges and partially curved or plane faces. The micrograph of the pristine alumina particles does not show any agglomerates which indicates a limited amount of adhesive forces between adjacent particles. Depending on the specific type, the median ranges between 14.5 µm and 44.1 µm. Additional particle species with a median of 0.5 µm and 5.5 µm, respectively, were used for preparation of the composite with the highest volume fractions, see Table 2. A scanning electron micrograph of the composite Al₂O₃-PVB 70.9 is presented in Fig. 3. After processing, the particles are uniformly distributed in the polymer component (see Fig. 3(a)) which is a consequence of the good mixing of the different material phases in the spouted bed spray granulation process [7]. The two different particle fractions with different average diameters can be clearly identified. The smaller particles with a median of approximately 0.5 µm are located in the void space between the larger particles (see arrow in Fig. 3). This arrangement yields a high filling degree. A close inspection of the surface of the large particles reveals the presence of a thin layer of PVB on the surface of the ceramic particles. This thin PVB layer seems to have a good adhesion to the surface of the inorganic particles. The fracture surface with a honeycomb-like structure indicates ductile failure with plastic deformation of the PVB phase.

The thermal stability (relative mass and its derivative as functions of temperature) of pristine poly(vinyl butyral) and the composite Al₂O₃-PVB 70.9 in argon atmosphere is shown in Fig. 4. The decomposition of pristine poly(vinyl butyral) starts at a temperature of approximately 310 °C. A second decomposition step appears at approximately 400 °C which can be anticipated in the high temperature shoulder of the dm/dT curve (derivative of relative mass) of PVB and more clearly seen in measurements which were performed in synthetic air [7]. The remaining ash content of poly(vinyl butyral) at 900 °C was 1.4 wt%. Figure 4 also presents the result of the thermal gravimetric analysis of the sample Al₂O₃-PVB 70.9. The start of decomposition of the PVB phase at a temperature of 310 °C can be clearly seen. At higher temperatures, the alumina particles are still stable. The remaining relative mass corresponds to the weight concentration of the composite. The volume fraction Φ of the ceramic particles was derived using $\Phi = \varphi \rho_{\text{sample}} / \rho_{\text{alumina}}$ with the weight fraction φ of the inorganic fillers, the measured density ρ_{sample} of the hot-pressed sample (i.e. after processing) and the density ρ_{alumina} of the ceramic particles.

At a heating rate of 1 K/min, the glass transition temperature of the composite Al₂O₃-PVB 70.9 was 66 °C, which is practically equal within experimental scatter to the T_g value of pristine PVB, cf. Table 1. Consequently, no statistically significant influence of the addition of ceramic fillers on the glass transition temperature of PVB was measured at our test parameters. In contrast to the work of Kirchberg et al. [4], the α -Al₂O₃ particles of this study have not been functionalized such that no influence (e.g., mixing effect) of a grafted polymer shell on the glass transition of the PVB phase exists.

The temperature dependence of the dynamic moduli G' and G'' of pristine poly(vinyl butyral) is shown in Fig. 5(a). Poly(vinyl butyral) depicts the viscoelastic properties of a polydisperse, amorphous thermoplastic polymer. Below the glass transition temperature, a predominantly elastic behavior with a storage modulus G' larger than the loss modulus G'' is observed (glassy behaviour). The glass transition is characterized by a pronounced decrease of the storage modulus and a maximum of the loss modulus. The experimental value (DMTA measurement) of the glass transition temperature (corresponding to the maximum of G'') is 63 °C. The small difference to the DSC result can be explained by different calibrations. In the temperature interval above the glass transition, the entanglement plateau can be identified by approximately constant values of G' . In the entanglement plateau, the values of G' are larger than the G'' values. At temperatures above 124 °C, the viscous properties dominate (G'' larger than G'), and the poly(vinyl butyral) melt is characterized by low values of the dynamic moduli. At a temperature of 150 °C, the zero shear rate viscosity η_0 of PVB is approximately $\eta_0 = 19\,000$ Pa s.

The dynamic moduli G' and G'' as a function of angular frequency ω are presented in Fig. 5(b) at a reference temperature of 60 °C. The results of frequency sweeps correspond to the temperature-dependent measurements. The glassy regime at high frequencies, transition zone, rubbery plateau and terminal flow zone at low frequencies can be clearly identified. The double intersections of storage and loss moduli result from glass transition and transition to terminal zone, respectively.

Figure 6(a) presents the dynamic moduli G' and G'' of pristine PVB and several ceramic-polymer composites as a function of temperature T . Below the glass transition temperature, the moduli of the ceramic-polymer composites are much larger than the corresponding moduli of pristine poly(vinyl butyral). An increasing filler concentration leads to an increase of storage and loss modulus. The significant increase of G'' (proportional to energy dissipation) at low temperatures can be explained by the friction (a dissipative process) between adjacent filler particles. With increasing particle concentration, the width of the maximum of G'' becomes larger which shows that a contribution in addition to the sole polymer phase to energy dissipation exists, namely by filler-filler and/or polymer-filler interactions. Above the glass transition temperature of poly(vinyl butyral), the ceramic-polymer composites still attain relatively large dynamic moduli which indicates the presence of an elastically deformable filler network (i.e. the contact network of particles) even at high temperatures. This effect shows that direct filler-filler interactions play a key role in the whole temperature range. The filler-filler interactions result from the contact forces between adjacent particles (cf. Fig. 6(b)). The total viscoelastic response is caused by filler-filler, polymer-filler and polymer-polymer interactions. However, the large enhancement of the storage modulus is mainly caused by filler-filler interactions. At high temperatures, the dynamic moduli of pristine poly(vinyl butyral) attain relatively low values. In this temperature range, the increase of the loss modulus of the composites in comparison to pristine poly(vinyl butyral) is caused by friction between adjacent fillers. The friction is also influenced by thin polymer layers between neighbouring particles. The reversibility of this test was checked by carrying out an immediately subsequent test for one sample with a cooling rate of 1 K/min which basically led to the same result. However, slight morphological changes most probably occur at temperatures near 150 °C which influence G'' of the composite below T_g of PVB.

The shear modulus G of pristine alumina is given by $G = 169 \text{ GPa} - 0.0229 \text{ GPa } ^\circ\text{C}^{-1} \times T$ [37] with the temperature T in °C. In a first step, we apply a phenomenological approach in order to describe the increase of modulus with filler loading and model the temperature-dependent storage modulus G' of the composite using a superposition of the parallel and the series model:

$$G' = a[\Phi G'_{\text{filler}} + (1 - \Phi)G'_{\text{polymer}}] + (1 - a)G'_{\text{filler}}G'_{\text{polymer}}/[\Phi G'_{\text{polymer}} + (1 - \Phi)G'_{\text{filler}}] \quad (1)$$

with the moduli G'_{polymer} and G'_{filler} of polymer and filler, respectively. Note that an analogous equation for G'' is not postulated in this study because the loss modulus G''_{filler} of the micron-sized particles could not be experimentally determined. The volume fraction of the filler particles is denoted by Φ . The (positive) mixing parameter a depends on temperature and frequency which was in this study $f = 1$ Hz. Equation (1) allows for evaluation of the measured modulus of the composite with respect to two limiting cases (parallel and series model). The value of a may be interpreted as follows: A low value of a shows that polymer-filler interactions play a significant role, since the series model can be associated with a polymer matrix surrounding the dispersed fillers and a force balance at the filler-polymer interface. A larger value of a indicates the dominance of the linear mixing rule (parallel model) which can be associated with a continuous filler phase. The high filler concentration of the composite of this work implies a morphology which, on the one hand, consists of fillers surrounded by a shell of polymer, but on the other hand also of chains of alumina particles in contact leading to a strong stiffness enhancement (the so-called contact network which consists of percolated particles, see Fig. 6(b)). In practice (i.e. for $G' < \Phi G'_{\text{filler}} + (1 - \Phi)G'_{\text{polymer}}$), the parameter a should range between zero and unity. The dependence of a on temperature T is shown in Fig. 6(c). In the temperature range from room temperature to the melt state of PVB, the parameter a decreases from approximately 0.1 to values close to zero above the glass transition temperature of poly(vinyl butyral). The relatively low value of 0.1 at low temperatures indicates only a limited number of chains of filler particles (and thus still a considerable number of non-percolated particles) which span the whole sample. In the limit of large values of $\kappa = G'_{\text{filler}}/G'_{\text{polymer}}$ (here $\kappa > 165$) we find from Eq. (1) $G' = [a\Phi\kappa + (1 - a)/(1 - \Phi)]G'_{\text{polymer}}$. Consequently, we find for $a \ll a_{\text{PM}} = 1/[1 + \kappa\Phi(1 - \Phi)]$ the dominance of the series model. In this work, we have $a \gg 1/[1 + \kappa\Phi(1 - \Phi)]$ for all composites in the whole temperature range which indicates the existence of an elastic contact network of alumina particles (parallel model), see also Fig. 6(c).

Figure 7 shows the reinforcement factors r_1 and r_2 for the storage and the loss modulus

$$r_1 = G'_{\text{composite}}/G'_{\text{polymer}} \quad (2)$$

$$r_2 = G''_{\text{composite}}/G''_{\text{polymer}} \quad (3)$$

as a function of temperature. Related enhancement factors as a function of angular frequency were previously introduced [38]. Both reinforcement factors strongly increase in the temperature interval up to 20-25 °C above the glass transition temperature of poly(vinyl butyral). A relative maximum of r_1 appears 8 – 15 °C above T_g which corresponds to the onset of the rubbery regime of pristine poly(vinyl butyral). At higher temperatures, the reinforcement factors r_1 and r_2 still increase, but in a less pronounced manner.

The value of r_2 also increases with filler concentration. At low temperatures below T_g of poly(vinyl butyral) r_2 ranges between 10 and 20. At a temperature of 60 °C, a minimum of r_2 appears which results from the shift of the maximum of G'' caused by the addition of fillers (cf. Fig. 6(a)). At a temperature of 140 °C the value of r_2 nearly is 1500 for the composite with the highest filler fraction which is lower than the value of $r_1 \approx 10\,000$ at the same temperature.

The influence of particle size on the dynamic moduli is presented in Fig. 8. Below the glass transition temperature T_g , the mixing effect does not depend on particle size. Above T_g , where the polymer chains are more mobile, a smaller particle size implies a larger surface to volume ratio. Therefore the total polymer-particle interface increases leading to a larger number of polymer-filler interactions. The polymer-filler interactions weaken the dynamic moduli above T_g , i.e. if the polymer chains are mobile. Consequently, a larger particle size (lower surface to volume ratio) implies larger dynamic moduli.

Since the poly(vinyl butyral) phase is associated with a viscoelastic response, at each temperature the values of the dynamic moduli depend on the applied angular frequency. Figure 9 presents the results of frequency sweeps at three selected temperatures (30, 90 and 120 °C) which correspond to the glassy state, the entanglement and to the crossover to the terminal flow regime, respectively. Each regime is associated with a different viscoelastic behaviour of the PVB matrix at the applied frequency of $f = 1$ Hz. The data in Fig. 9 convincingly demonstrate the existence of polymer-filler interactions. At 30 °C and 90 °C, the PVB matrix is characterized by a predominantly elastic behaviour with a larger loss modulus at 90 °C than at 30 °C. At a temperature of 120 °C, the PVB matrix acts like a viscoelastic fluid with a strong frequency dependence of the dynamic moduli. At a temperature of 30 °C, the loss modulus of the ceramic-polymer composite decreases with frequency which can be interpreted by the influence of Coulomb friction between two neighboured ceramic particles. Above the glass transition temperature of poly(vinyl butyral) the network of filler particles becomes weaker, see the data at 90 °C. An increasing temperature leads to volume expansion, a higher mobility and thus a

larger deformation of the polymer phase which results in an increase of the average particle distance and possibly to the decrease of filler-filler interactions. Even at a temperature of 120 °C, the ceramic-polymer composite attains relatively large dynamic moduli. Such large moduli can be explained by the presence of a large amount of elastic filler-filler interactions. The value of the storage modulus G' of the composite with the highest concentration of ceramic fillers is nearly independent on the angular frequency which indicates the formation of an elastically deformable network of filler particles (direct filler-filler contacts). The absolute value of the storage modulus G' decreases with temperature, which shows that the elastic network is also strongly influenced by the polymer phase. Generally, a larger particle size yields higher values of the storage modulus, cf. also Fig. 8. The curve in Fig. 9(c) clearly demonstrates that two different contributions to the network exist, namely direct filler-filler contacts (which depend to a lesser extent on temperature) and polymer-filler interactions which are broken up at a certain temperature.

The influence of the deformation amplitude γ_0 was studied by performing oscillatory amplitude sweeps in the range $\gamma_0 = 0.02\% - 0.2\%$. Such an analysis gives much insight into the influence of morphology on the viscoelastic properties [39]. The data of the dynamic moduli as a function of strain amplitude are depicted in Fig. 10 at several temperatures, i.e. below and above the glass transition temperature of poly(vinyl butyral). The data for the tests which were performed below the glass transition temperature of the poly(vinyl butyral) phase indicate the breakup of a network at extremely low values of strain. Even at strain amplitudes up to $\gamma_0 = 0.05\%$ a slight decrease of the storage modulus G' can be detected. On the contrary, the loss modulus G'' slightly increases with strain amplitude. The increase of energy dissipation (increase of loss modulus G'') can be explained by the rupture of filler-filler bonds. At the test temperature of 90 °C the relative decrease of the storage modulus with shear amplitude is more pronounced than at the test temperature of 30 °C. In contrast to the measurements at 30 °C, the loss modulus G'' decreases with γ_0 at 90 °C. At a temperature of 90 °C and higher temperatures, the polymer chains are partially mobile such that a higher strain amplitude leads to a decrease of entanglements. Generally, the storage modulus G' continuously decreases with temperature which indicates the high relevance of the polymer phase for the filler-filler interactions. This trend is seen in Fig. 10. Since G'' attains a maximum near the glass transition temperature, G'' does not decrease monotonically with temperature in Fig. 10.

Finally, we report on the time-temperature superposition principle for pristine poly(vinyl butyral) and the composites. The application of the principle which is well established for amorphous thermoplastic homopolymers was satisfactorily applied to

the homopolymer and the highly-filled composite Al₂O₃-PVB 70.9 using the software LSSHIFT [40], see Fig. 11. The frequency range spans 20 powers of ten. Figure 11(a) reveals that the ceramic-polymer composite is characterized by a predominantly elastic behavior in the whole experimentally accessible frequency range. The relative maximum of G'' is shifted towards lower frequencies when comparing the composite with pristine poly(vinyl butyral). This result indicates that filler-filler and polymer-filler interactions strongly contribute to dissipation during deformation and not only the PVB phase itself, see also the comparison of the data measured at a temperature of 60 °C (Fig. 11(b)). The master curve also reveals that below the glass transition temperature (i.e. in the high frequency range) of poly(vinyl butyral) Coulomb friction takes place, since the value of G'' of the composite is much larger than the loss modulus of pristine poly(vinyl butyral).

The shift factor a_T follows from the Williams-Landel-Ferry equation:

$$\log(a_T) = -\frac{c_1(T-T_{\text{ref}})}{c_2+T-T_{\text{ref}}} \quad (4)$$

with the reference temperature T_{ref} and the material specific parameters c_1 and c_2 . A least squares-fit yields the values $c_1 = 14.6 \pm 0.9$ and $c_2 = 41.1 \text{ K} \pm 5.6 \text{ K}$ for pristine poly(vinyl butyral) and $c_1 = 15.5 \pm 1.1$ and $c_2 = 36.6 \text{ K} \pm 4.9 \text{ K}$ for the composite Al₂O₃-PVB 70.9 ($T_{\text{ref}} = 60 \text{ °C}$). Below the glass transition temperature of poly(vinyl butyral), the shift factor only moderately decreases with temperature (Fig. 11(c)) and a temperature shift influences the mobility of the polymer chains to a lower extent, see also the data for polystyrene in the work of Schwarzl and Zahrádník [41].

The results of dielectric measurements are shown in Figs. 12 and 13. Generally, the complex dielectric constant $\varepsilon^*(\omega) = \varepsilon'(\omega) - i\varepsilon''(\omega)$ is written as

$$\varepsilon^*(\omega) = \varepsilon'(\omega) - i[\varepsilon_{\text{diel}}''(\omega) + \sigma_0/(\varepsilon_0\omega)] \quad (5)$$

with the angular frequency $\omega = 2\pi f$, the frequency f measured in Hz, the dielectric contribution $\varepsilon_{\text{diel}}''$ to the dielectric loss ε'' and the direct current electrical conductivity σ_0 . The permittivity constant is denoted by ε_0 . The dielectric properties of thin films of alumina were measured by Argall and Jonscher [42] and Prasanna et al. [43].

The results of isothermal measurements at temperatures of 60, 70 and 80 °C are presented in Fig. 12. Below its glass transition temperature of 65 °C pristine poly(vinyl butyral) is characterized by an almost constant value of ε' (behavior of an isolator). At higher temperatures, the stepwise decrease of ε' with ω corresponding to the glass transition can be seen. The dielectric loss ε'' of pristine poly(vinyl butyral) is associated with a maximum (glass transition). A different behavior is observed for the

composite Al₂O₃-PVB 70.9. At low frequencies, the value of ϵ' increases with decreasing frequency. The maximum of ϵ'' which appears for PVB at a frequency of $f \approx 130$ Hz at 80 °C and corresponds to the glass transition of the PVB phase can be also anticipated in the curve of the composite Al₂O₃-PVB 70.9. Therefore the spectrum of the composite agrees with the calorimetric glass transition temperatures which indicate similar T_g values of PVB in the pristine PVB and in the composite. Note that the position of the maximum results from the superposition of the contributions of the PVB phase and the alumina particles. The low frequency response possibly results from trapped space charges at the ceramic-polymer interface (Maxwell-Wagner-Sillars (MWS) effect) [44]. Furthermore, Fig. 12(b) reveals a secondary relaxation in the composite at a temperature of 60 °C and a frequency of approximately 10 kHz. The origin of this secondary relaxation peak is open. The data of the dielectric measurements clearly reveal that the ceramic component strongly contributes to the dielectric permittivity (mixing effect) in the whole investigated frequency range. The increase of the dielectric permittivity for the composite is only moderate because of the relatively low dielectric permittivity of alumina. A large increase in the value can be expected when other ceramics with high dielectric permittivities such as BaTiO₃ are used as inorganic filler material. The alternating current (ac) conductivity $\sigma' = \omega \epsilon_0 \epsilon''$ of the composite scales with the power law exponent 0.89 at large frequencies and a temperature of 70 °C. This power-law exponent has been also found by other researchers for thin alumina films [43].

Figure 13 presents the real and the imaginary part of the permittivity at a frequency $f = 100$ Hz as a function of temperature. The maximum of the dielectric loss ϵ'' is associated with the glass transition. The temperature which is associated with the maximum of the dielectric loss is higher than the measured calorimetric glass transition temperature by the DSC method, since the applied frequency of 100 Hz probes shorter time scales than the DSC measurements. Comparing the data of pristine poly(vinyl butyral) and the composite and taking into account the contribution of the Al₂O₃ phase to ϵ'' , no significant change of the glass transition temperature within experimental resolution can be detected. Consequently, the dielectric measurements support the result of the DSC experiments.

4. Conclusions

In this study, the influence of temperature on the viscoelastic properties of composites of poly(vinyl butyral) and α -Al₂O₃ particles was investigated. Application of the spouted bed spray granulation process and subsequent hot-pressing allows achieving filler fractions above 70 vol%. At such high filler fractions, a large number of direct filler-filler contacts exist. The rheological experiments clearly show that both

direct filler-filler contacts and polymer-filler interactions contribute to the elastic response of the composites. The reinforcement effect caused by the ceramic filler particles is strongly pronounced in the temperature interval above the glass transition temperature of the poly(vinyl butyral) phase. Our data show that the reinforcement factor of the storage modulus attains values up to four orders of magnitude in the temperature range above the glass transition temperature of poly(vinyl butyral). For specimens with the highest filling degree the value of G' at temperatures 50 °C above T_g was still larger than the value of G' at room temperature for the unfilled polymer. Consequently, the softening of the polymer above T_g is effectively averted. This effect increases the maximum service temperature of polymers, which is a limiting factor for many applications and can be increased by a high filling degree.

The relative contribution of filler-filler and polymer-filler interactions can be described by a phenomenological equation which implies a linear superposition of the parallel and the series model. If the concentration of inorganic particles is constant, smaller particles imply a larger contribution of polymer-filler interactions than larger particles, an effect which leads above T_g to a lower storage modulus for composites with smaller particles at constant filler concentration.

Generally, the addition of alumina to poly(vinyl butyral) increases the permittivity. However, the differential scanning calorimetry and dielectric data show no significant shift of the value of the glass transition temperature of poly(vinyl butyral) within experimental scatter. In these composites with micron-sized fillers, the glass transition temperature of the polymer component is not affected by the presence of the ceramic particles.

Acknowledgement

We gratefully acknowledge financial support from the German Research Foundation (DFG) via SFB 986 "M3", projects A2 and A3. The authors thank Clarissa Abetz for scanning electron microscopy (SEM) investigations, Maren Brinkmann for gel permeation chromatography (GPC) measurements and Ivonne Ternes for differential scanning calorimetry (DSC) measurements and thermal gravimetric analysis (TGA).

References

- [1] M.F. Ashby, Y.J.M. Bréchet, Designing hybrid materials, *Acta Materialia*, 51 (2003) 5801-5821.
- [2] S. Bechtle, S.F. Ang, G.A. Schneider, On the mechanical properties of hierarchically structured biological materials, *Biomaterials*, 31 (2010) 6378-6385.
- [3] A.R. Studart, Towards high-performance bioinspired composites, *Advanced Materials*, 24 (2012) 5024-5044.
- [4] S. Kirchberg, M. Rudolph, G. Ziegmann, U.A. Peuker, Nanocomposites based on technical polymers and sterically functionalized soft magnetic magnetite nanoparticles: Synthesis, processing, and characterization, *Journal of Nanomaterials*, (2012) Article ID 670531.
- [5] S. Kirchberg, M. Anhalt, G. Ziegmann, Theoretical consideration of experimental data of thermal and magnetic properties of polymer-bonded soft magnetic composites, *Journal of Thermoplastic Composite Materials*, 27 (2014) 663-678.
- [6] L. Xie, S. Kirchberg, M. Rudolph, G. Ziegmann, U. Peuker, Effect of compounding principles on thermal, mechanical and magnetic performance of soft magnetic polymethylmethacrylate/Fe₃O₄ nanocomposites, *Journal of Reinforced Plastics and Composites*, 32 (2013) 1928-1933.
- [7] M.F.H. Wolff, V. Salikov, S. Antonyuk, S. Heinrich, G.A. Schneider, Novel, highly-filled ceramic-polymer composites synthesized by a spouted bed spray granulation process, *Composites Science and Technology*, 90 (2014) 154-159.
- [8] K. Brandt, C. Neusel, S. Behr, G.A. Schneider, Dielectric behaviour and conductivity of high-filled BaTiO₃-PMMA composites and the facile route of emulsion polymerization in synthesizing the same, *Journal of Materials Chemistry C*, 1 (2013) 3129-3137.
- [9] K. Brandt, M.F.H. Wolff, V. Salikov, S. Heinrich, G.A. Schneider, A novel method for a multi-level hierarchical composite with brick-and-mortar structure, *Scientific Reports*, 3 (2013) 2322-2329.
- [10] C.M. Roland, Dynamic mechanical behavior of filled rubber at small strains, *Journal of Rheology*, 34 (1990) 25-34.
- [11] C.F. Schmid, L.H. Switzer, D.J. Klingenberg, Simulations of fiber flocculation: Effects of fiber properties and interfiber friction, *Journal of Rheology*, 44 (2000) 781-809.
- [12] M. Simhambhatla, A.I. Leonov, On the rheological modeling of filled polymers with particle-matrix interactions, *Rheologica Acta*, 34 (1995) 329-338.
- [13] H.A. Barnes, A review of the rheology of filled viscoelastic systems, *Rheology Reviews*, (2003) 1-36.
- [14] P. Pötschke, M. Abdel-Goad, I. Alig, S. Dudkin, D. Lellinger, Rheological and dielectrical characterization of melt mixed polycarbonate-multiwalled carbon nanotube composites, *Polymer*, 45 (2004) 8863-8870.
- [15] D.S. Bangarusampath, H. Ruckdäschel, V. Altstädt, J.K.W. Sandler, D. Garray, M.S.P. Shaffer, Rheological and electrical percolation in melt-processed poly(ether ether ketone)/multi-wall carbon nanotube composites, *Chemical Physics Letters*, 482 (2009) 105-109.
- [16] D.S. Bangarusampath, H. Ruckdäschel, V. Altstädt, J.K.W. Sandler, D. Garray, M.S.P. Shaffer, Rheology and properties of melt-processed poly(ether ether ketone)/multi-wall carbon nanotube composites, *Polymer*, 50 (2009) 5803-5811.
- [17] U.A. Handge, K. Hedicke-Höchstötter, V. Altstädt, Composites of polyamide 6 and silicate nanotubes of the mineral halloysite: Influence of molecular weight on thermal, mechanical and rheological properties, *Polymer*, 51 (2010) 2690-2699.
- [18] R. Zeiler, U.A. Handge, D.-J. Dijkstra, H. Meyer, V. Altstädt, Influence of molar mass and temperature on the dynamics of network formation in polycarbonate/carbon nanotubes composites in oscillatory shear flows, *Polymer*, 52 (2011) 430-442.
- [19] S. Rooj, A. Das, K.W. Stöckelhuber, D.-Y. Wang, V. Galiatsatos, G. Heinrich, Understanding the reinforcing behavior of expanded clay particles in natural rubber compounds, *Soft Matter*, 9 (2013) 3798-3808.
- [20] E. Guth, E. Gold, On the hydrodynamical theory of the viscosity of suspensions, *Physical Review*, 53 (1938) 322-324.

- [21] E. Guth, Theory of filler reinforcement, *Journal of Applied Physics*, 16 (1945) 20-25.
- [22] H.M. Smallwood, Limiting law of the reinforcement of rubber, *Journal of Applied Physics*, 15 (1944) 758-766.
- [23] M.I. Aranguren, E. Mora, J. Jon V. DeGroot, C.W. Macosko, Effect of reinforcing fillers on the rheology of polymer melts, *Journal of Rheology*, 36 (1992) 1165-1182.
- [24] D.M. Bigg, Rheological behaviour of highly filled polymer melts, *Polymer Engineering and Science*, 23 (1983) 206.
- [25] D.R. Saini, A.V. Shenoy, V.M. Nadkarni, Melt rheology of highly-loaded ferrite-filled polymer composites, *Polymer Composites*, 7 (1986) 193-200.
- [26] P. Cassagnau, Linear viscoelasticity and dynamics of suspensions and molten polymers filled with nanoparticles of different aspect ratios, *Polymer*, 54 (2013) 4762-4775.
- [27] J.C. Halpin, J.L. Kardos, Moduli of crystalline polymers employing composite theory, *Journal of Applied Physics*, 43 (1972) 2235-2241.
- [28] J.C. Halpin, J.L. Kardos, The Halpin-Tsai equations: A review, *Polymer Engineering and Science*, 16 (1976) 344-352.
- [29] A.R. Payne, The dynamic properties of carbon black-loaded natural rubber vulcanizates. Part I, 1962, 6 (1962) 57-63.
- [30] G. Heinrich, M. Klüppel, Recent advances in the theory of filler networking in elastomers, *Advances in Polymer Sciences*, 160 (2002) 1-44.
- [31] M. Klüppel, The role of disorder in filler reinforcement of elastomers on various length scales, *Advances in Polymer Sciences*, 164 (2003) 1-86.
- [32] G. Heinrich, F.R. Costa, M. Abdel-Goad, U. Wagenknecht, B. Lauke, V. Härtel, J. Tschimmel, M. Klüppel, A.L. Svistkov, Structural kinetics in filled elastomers and PE/LDH composites, *Kautschuk Gummi Kunststoffe*, 58 (2005) 163-167.
- [33] C.-C. Peng, A. Göpfert, M. Drechsler, V. Abetz, "Smart" silica-rubber nanocomposites in virtue of hydrogen bonding interaction, *Polymers for Advanced Technologies*, 16 (2005) 770-782.
- [34] M.M. Kummali, L.A. Miccio, G.A. Schwartz, A. Alegría, J. Colmenero, J. Otegui, A. Petzold, S. Westermann, Local mechanical and dielectric behavior of the interacting polymer layer in silica nanoparticles filled SBR by means of AFM-based methods, *Polymer*, 54 (2013) 4980-4986.
- [35] J. Otegui, G.A. Schwartz, S. Cervený, J. Colmenero, J. Loichen, S. Westermann, Influence of water and filler content on the dielectric response of silica-filled rubber compounds, *Macromolecules*, 46 (2013) 2407-2416.
- [36] KurarayEuropeGmbH, Technical Data Sheet, (2012).
- [37] R.G. Munro, Evaluated material properties for a sintered alpha-alumina, *Journal of the American Ceramical Society*, 80 (1997) 1919-1928.
- [38] U.A. Handge, P. Pötschke, Deformation and orientation during shear and elongation of a polycarbonate/carbon nanotubes composite in the melt, *Rheologica Acta*, 46 (2007) 889-898.
- [39] L. Tzounis, S. Debnath, S. Roj, D. Fischer, E. Mäder, A. Das, M. Stamm, G. Heinrich, High performance natural rubber composites with a hierarchical reinforcement structure of carbon nanotube modified natural fibers, *Materials and Design*, 58 (2014) 1-11.
- [40] J. Honerkamp, J. Weese, A note on estimating mastercurves, *Rheologica Acta*, 32 (1993) 57-64.
- [41] F.R. Schwarzl, F. Zahrádnik, The time temperature position of the glass-rubber transition of amorphous polymers and the free volume, *Rheologica Acta*, 19 (1980) 137-152.
- [42] F. Argall, A.K. Jonscher, Dielectric properties of thin films of aluminium oxide and silicon oxide, *Thin Solid Films*, 2 (1968) 185-210.
- [43] S. Prasanna, G.M. Rao, S. Jayakumar, M.D. Kannan, V. Ganesan, Dielectric properties of DC reactive magnetron sputtered Al₂O₃ thin films, *Thin Solid Films*, 520 (2012) 2689-2694.
- [44] A. Peláiz-Barranco, Modeling of dielectric relaxation response of ceramic/polymer composite based on lead titanate, *Scripta Materialia*, 54 (2006) 47-50.

Table Captions

Table 1: Physical properties of poly(vinyl butyral). The number-average M_n and the weight-average M_w of the molecular weight were determined by gel permeation chromatography (calibration using polystyrene standard). The glass transition temperature T_g of PVB was measured using differential scanning calorimetry in a nitrogen atmosphere. The analysis is based on the second heating interval. The heating rate is indicated. The value of T_g as determined by DMTA measurements at a frequency of $f = 1$ Hz is also listed.

Table 2: Composition of ceramic-polymer composites of this study. The polymer component is poly(vinyl butyral) Mowital® B 30 H. The volume fraction and the diameter of α -Al₂O₃ particles are indicated. A bimodal particle size distribution (type 1 and type 2 particles) was necessary for preparation of highly filled ceramic-polymer composites.

Tables

| Polymer | Supplier | M_n (g/mol) | M_w (g/mol) | PDI | T_g (°C) DSC 10 K/min | T_g (°C) DSC 1 K/min | T_g (°C) DMTA 1 K/min $f = 1$ Hz |
|--|---|------------------|------------------|-----|----------------------------------|---------------------------------|--|
| Poly(vinyl butyral) Mowital® B 30 H | Kuraray Specialities Europe GmbH | 37 200 | 87 600 | 2.4 | 68 | 65 | 63 |

Table 1

| Material | Particle concentration (vol%) | Median $d_{50,3}$ of particle diameter (type 1) (μm) | Median $d_{50,3}$ of particle diameter (type 2) (μm) |
|--|--------------------------------------|--|--|
| PVB | 0.0 | - | - |
| Al ₂ O ₃ -PVB 60.9 | 60.9 | 14.5 | - |
| Al ₂ O ₃ -PVB 61.1 | 61.1 | 18.2 | - |
| Al ₂ O ₃ -PVB 62.3 | 62.3 | 44.1 | - |
| Al ₂ O ₃ -PVB 67.1 | 67.1 | 26.3 | 5.5 |
| Al ₂ O ₃ -PVB 70.9 | 70.9 | 26.3 | 0.5 |
| Al ₂ O ₃ -PVB 76.5 | 76.5 | 26.3 | 0.5 |

Table 2

Figure Captions

Figure 1: Scheme of the spouted bed spray granulation process for preparation of highly filled ceramic-polymer composites.

Figure 2: Scanning electron micrograph of alumina particles (α -Al₂O₃) of this study.

Figure 3: Scanning electron micrographs of a composite of poly(vinyl butyral) and α -Al₂O₃ particles with a volume concentration of 70.9% (bimodal particle size distribution) using different magnifications ((a) – (c)).

Figure 4: Results of thermal gravimetric analysis (TGA) using pristine poly(vinyl butyral) and an α -Al₂O₃/PVB composite with a volume concentration of 70.9% ceramic particles. The heating rate was 10 K/min and an argon atmosphere was applied.

Figure 5: Viscoelastic properties of poly(vinyl butyral) Mowital® B 30 H. (a) Storage modulus G' and loss modulus G'' as a function of temperature T at a frequency of $f = 1$ Hz and a heating/cooling rate 1 K/min. The data below 72 °C were determined using a torsion geometry. The data above 72 °C were determined using a plate-plate geometry. (b) Master curve for the storage modulus G' and the loss modulus G'' as a function of angular frequency ω at a reference temperature of $T_{\text{ref}} = 60$ °C.

Figure 6: (a) Results of dynamic-mechanical thermal analysis for Al₂O₃-PVB composites with different particle concentrations at a frequency of $f = 1$ Hz. The heating rate was 1 K/min. The measurements were performed in a nitrogen atmosphere. (b) Scheme of the morphology of a highly filled composite with particles surrounded by a polymer shell and a chain of particles being in contact. (c) Value of the parameter a (see Eq. (1)) as a function of temperature T based on the data in Fig. 6(a). The value of a_{PM} (dashed line) corresponds to a volume fraction of $\Phi = 0.609$.

Figure 7: (a) Reinforcement factors r_1 and (b) r_2 (see Eqs. (2) and (3)) as a function of temperature T and concentration of the ceramic-polymer composites in Fig. 6(a). The values of r_1 and r_2 were determined based on the data for $f = 1$ Hz.

Figure 8: Influence of particle size (indicated in brackets) on the dynamic moduli G' and G'' . The frequency was $f = 1$ Hz, the amplitude of shear strain 0.05% and the heating rate 1 K/min. The particle concentration was approximately 61 vol%.

Figure 9: Dynamic moduli G' and G'' as a function of angular frequency ω at a measurement temperature of (a) 30 °C, (b) 90 °C and (c) 120 °C. The particle concentration is indicated.

Figure 10: (a) Storage modulus G' and (b) loss modulus G'' determined by amplitude sweeps for the composite Al_2O_3 -PVB 70.9 at different temperatures. The measurement temperatures are indicated. The angular frequency was $\omega = 10$ rad/s.

Figure 11: (a) Master curve of the dynamic moduli G' and G'' for pristine poly(vinyl butyral) and the composite Al_2O_3 -PVB 70.9 at a reference temperature of 60 °C. (b) Data of individual measurements at a temperature of 60 °C. (c) Shift factor a_T as a function of temperature T . The reference temperature is $T_{\text{ref}} = 60$ °C. The dashed and dotted lines correspond to the WLF equation (4) (see text for fit parameters).

Figure 12: (a) Real and (b) imaginary part ε' and ε'' of the complex permittivity $\varepsilon^*(\omega)$ with $\omega = 2\pi f$ for pristine poly(vinyl butyral) and the composite Al_2O_3 -PVB 70.9 determined by isothermal dielectric broadband spectroscopic measurements. The test temperature is indicated.

Figure 13: (a) Real and (b) imaginary part ε' and ε'' of the complex permittivity ε^* for $f = 100$ Hz as a function of temperature T for pristine poly(vinyl butyral) and the composite Al_2O_3 -PVB 70.9.

Figures

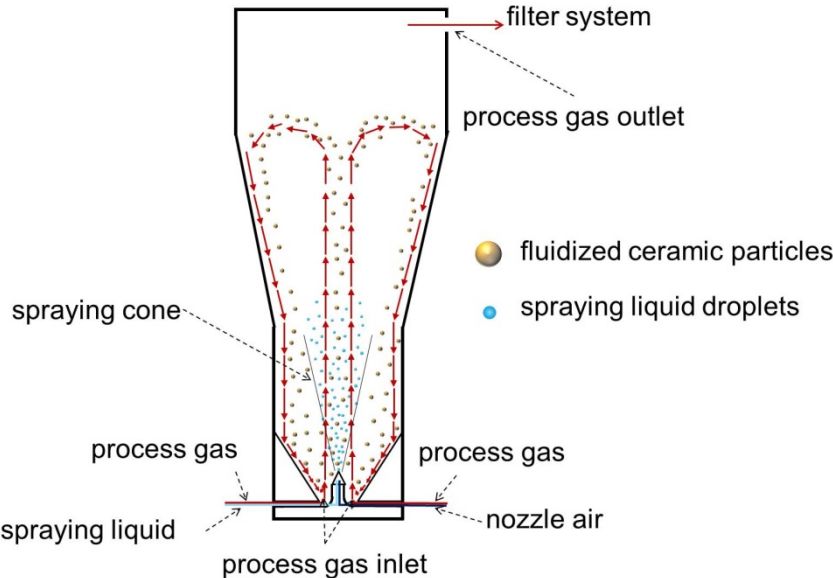


Figure 1
U.A. Handge et al.
Polymer

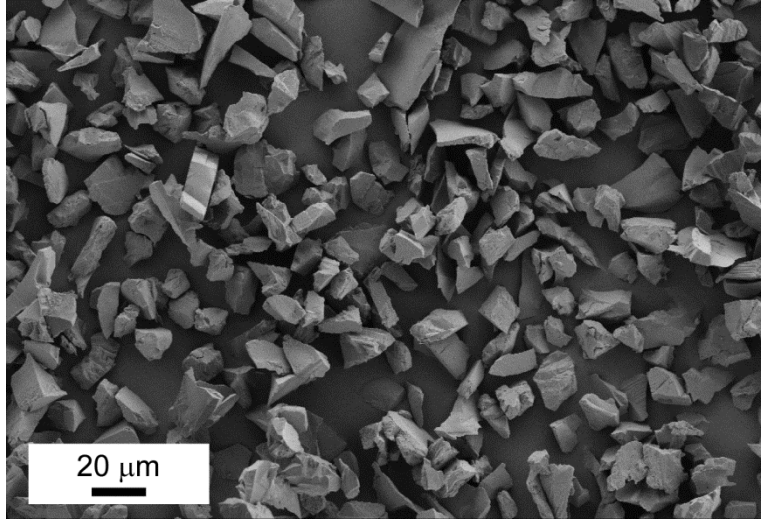


Figure 2

U.A. Handge et al.

Polymer

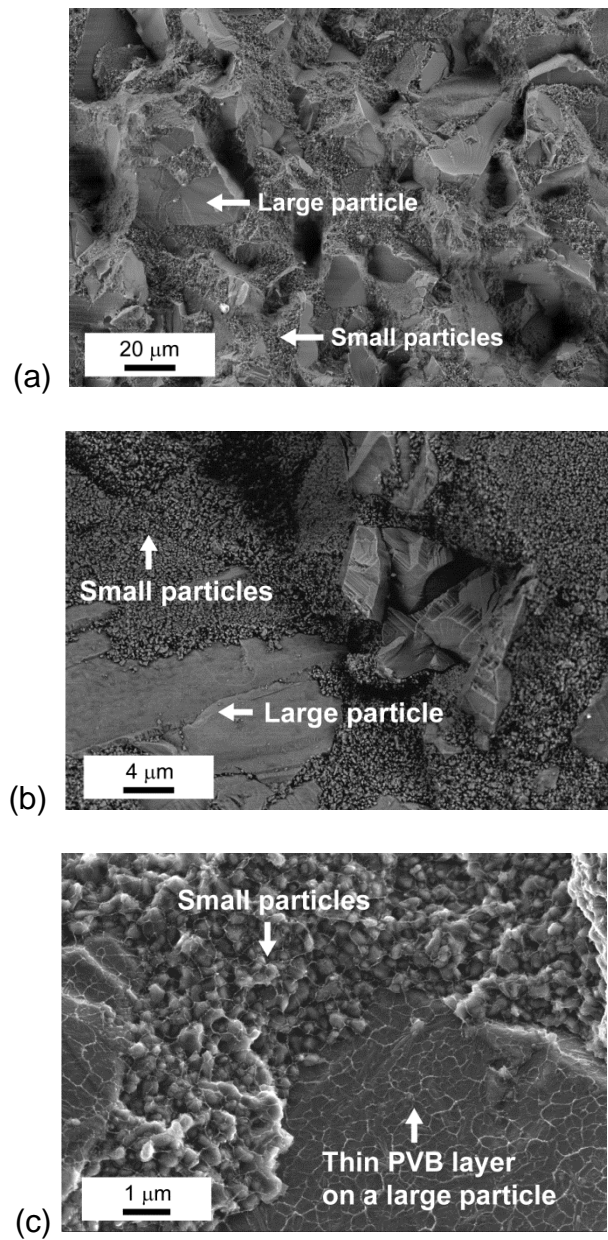


Figure 3
U.A. Handge et al.
Polymer

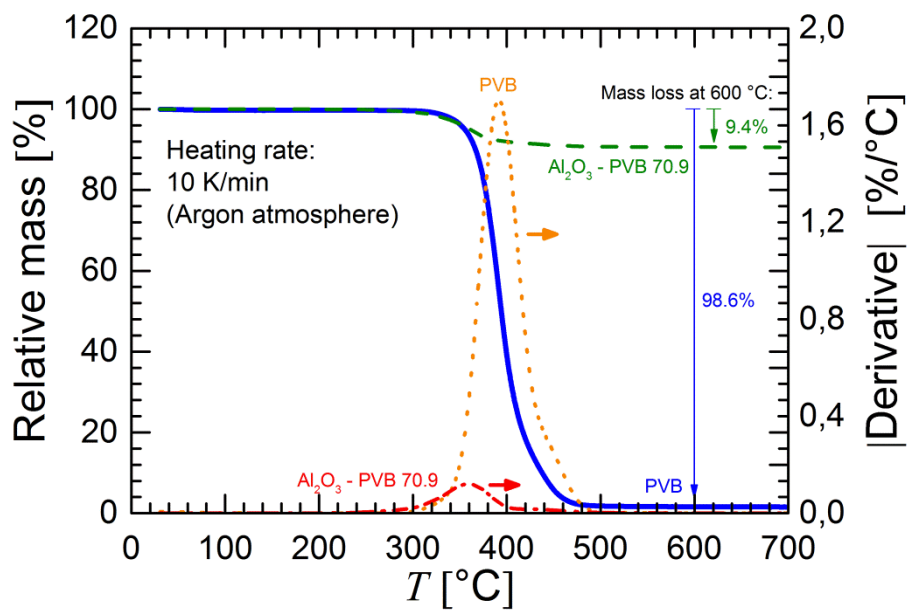
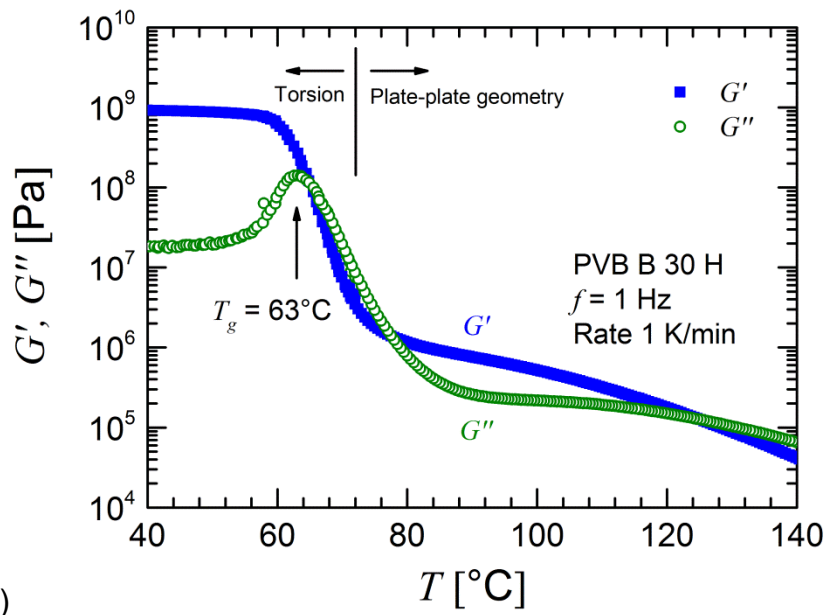


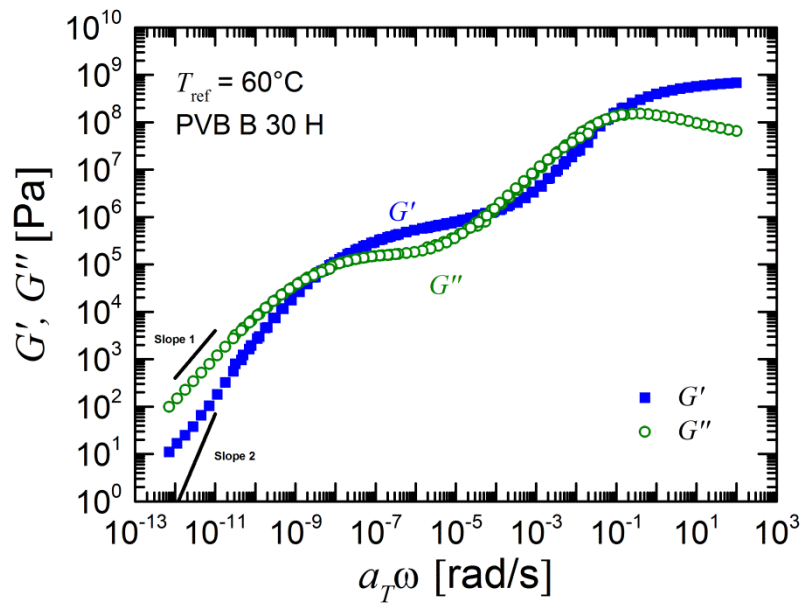
Figure 4

U.A. Handge et al.

Polymer



(a)

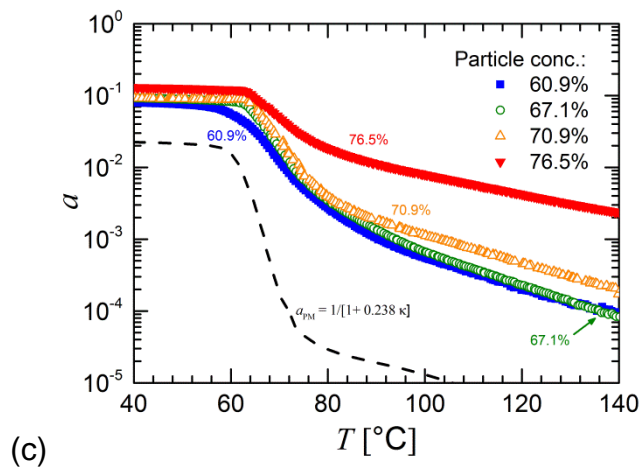
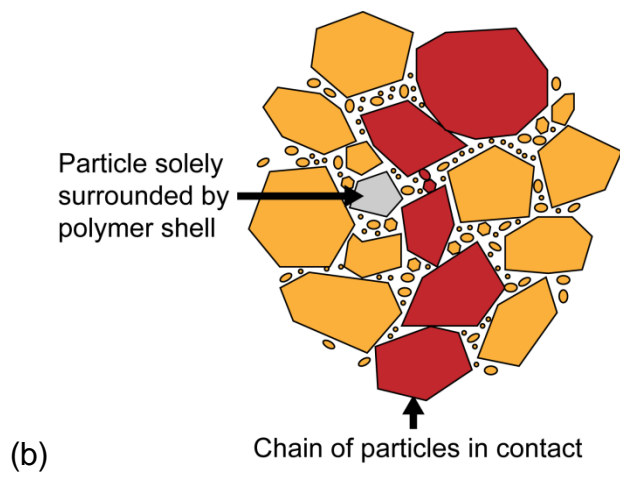
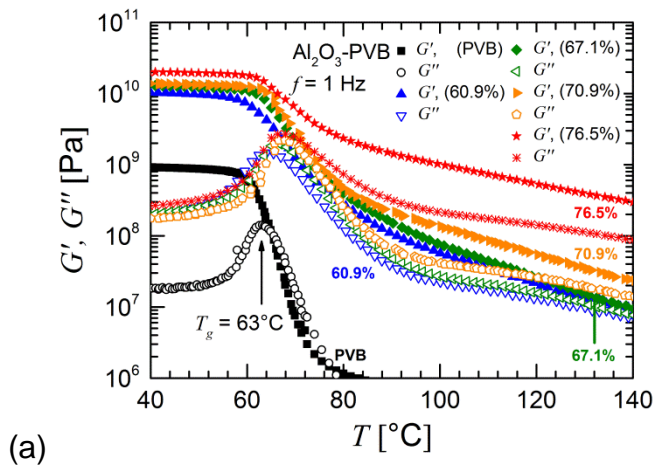


(b)

Figures 5(a) and (b)

U.A. Handge et al.

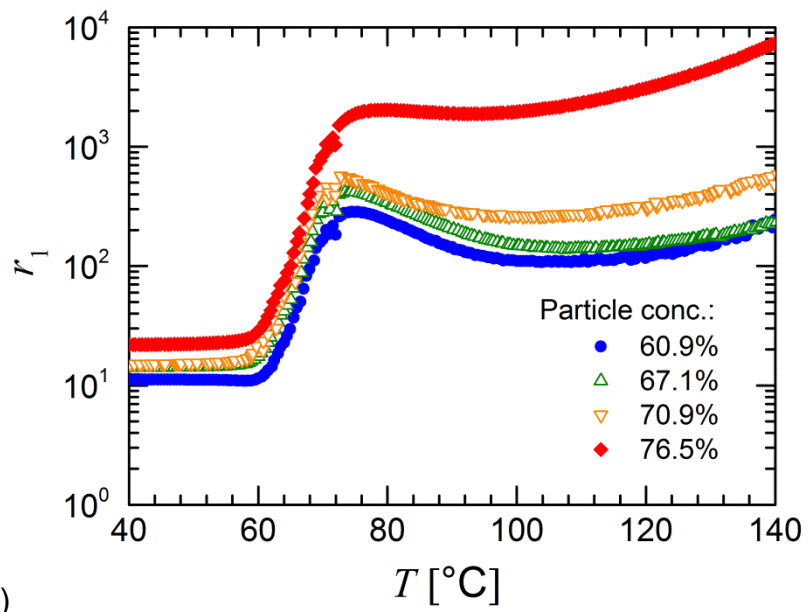
Polymer



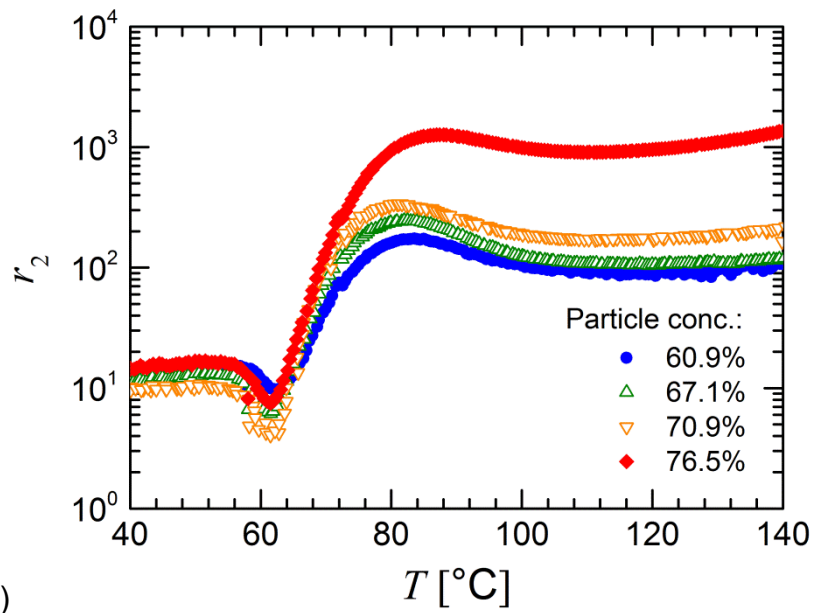
Figures 6(a) to (c)

U.A. Handge et al.

Polymer



(a)



(b)

Figures 7(a) and (b)

U.A. Handge et al.

Polymer

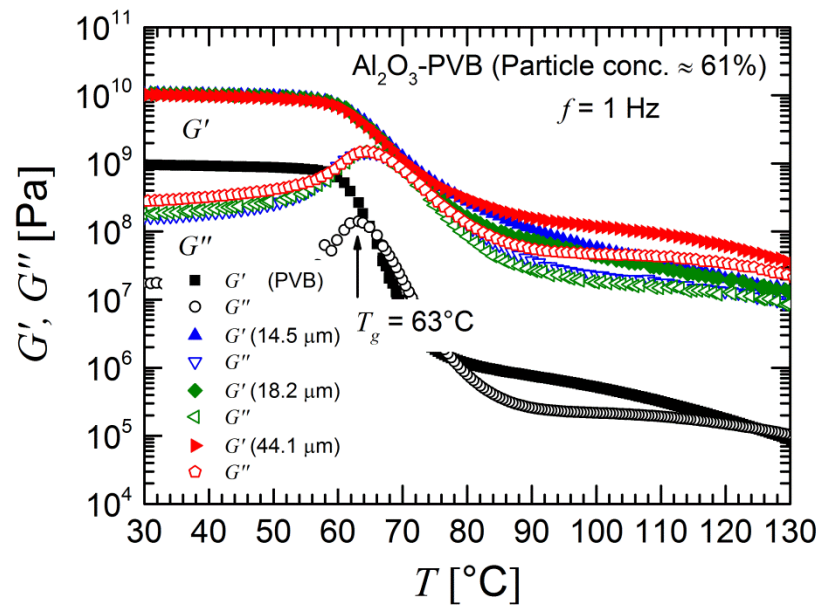
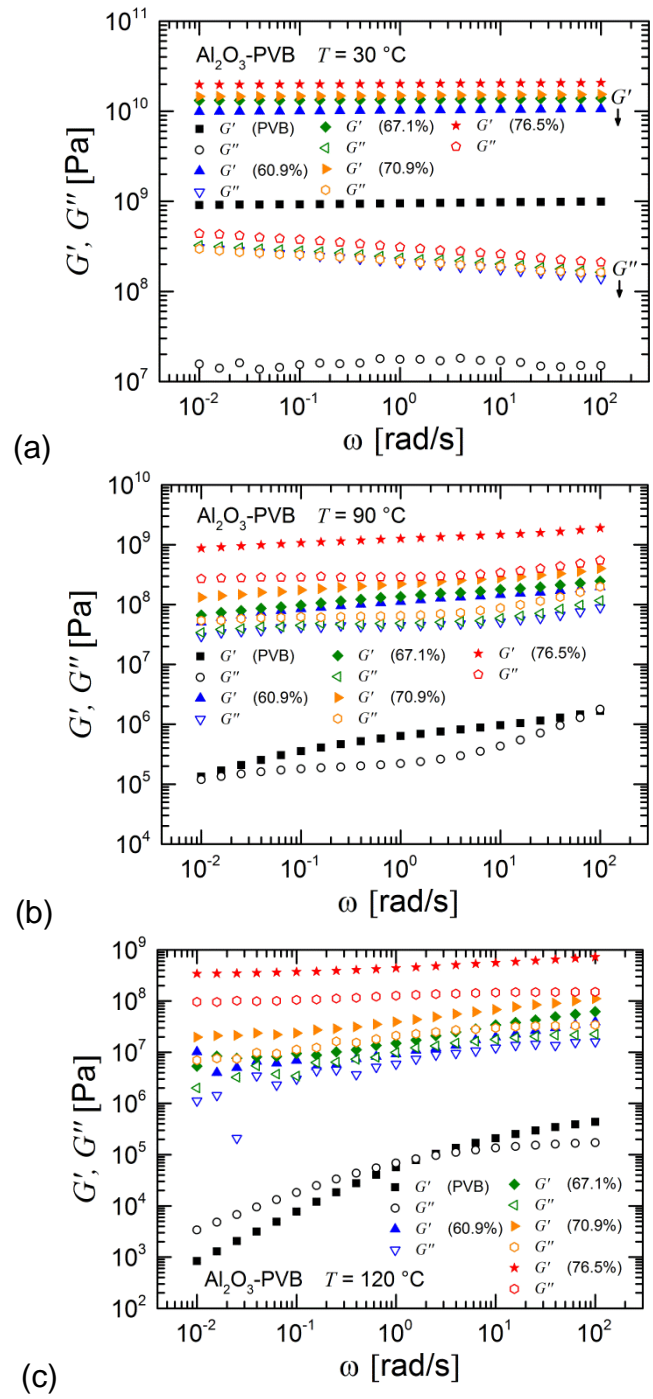


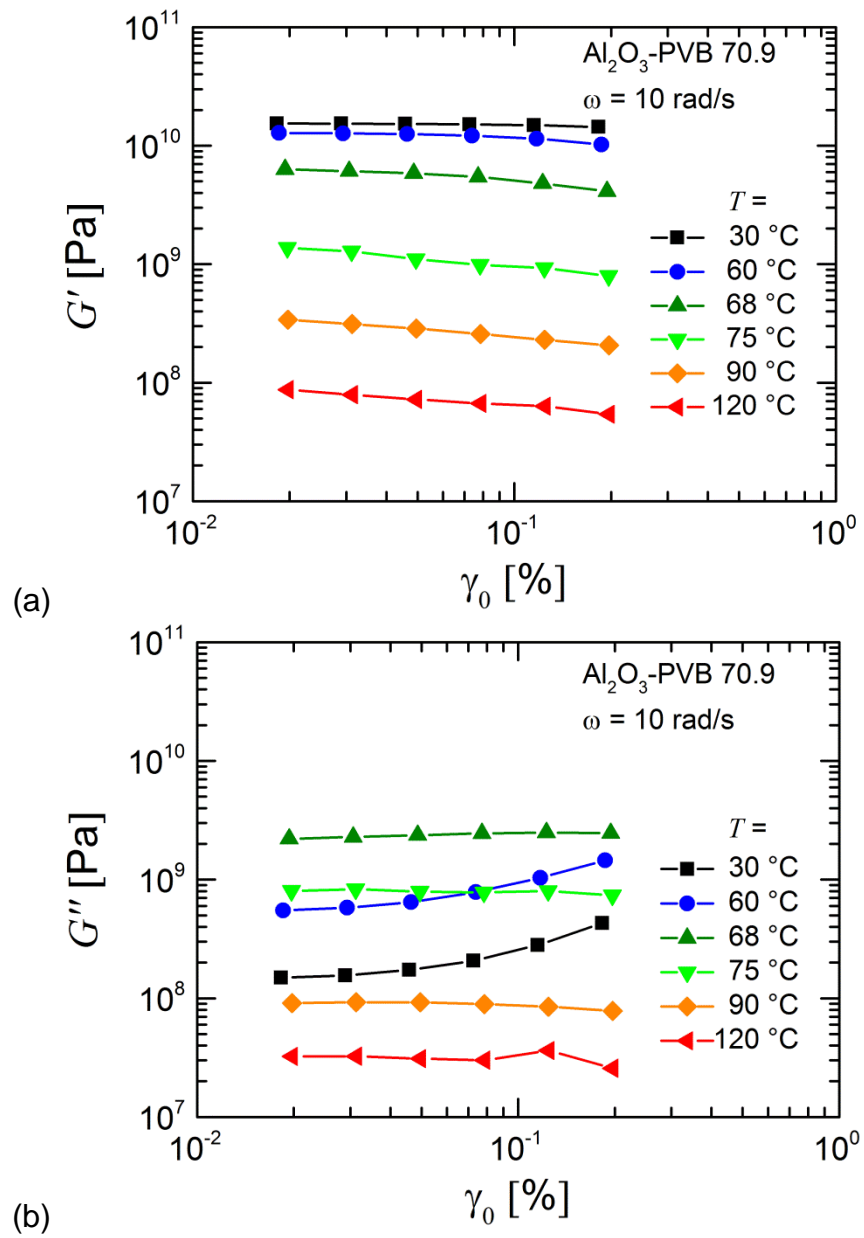
Figure 8

U.A. Handge et al.

Polymer



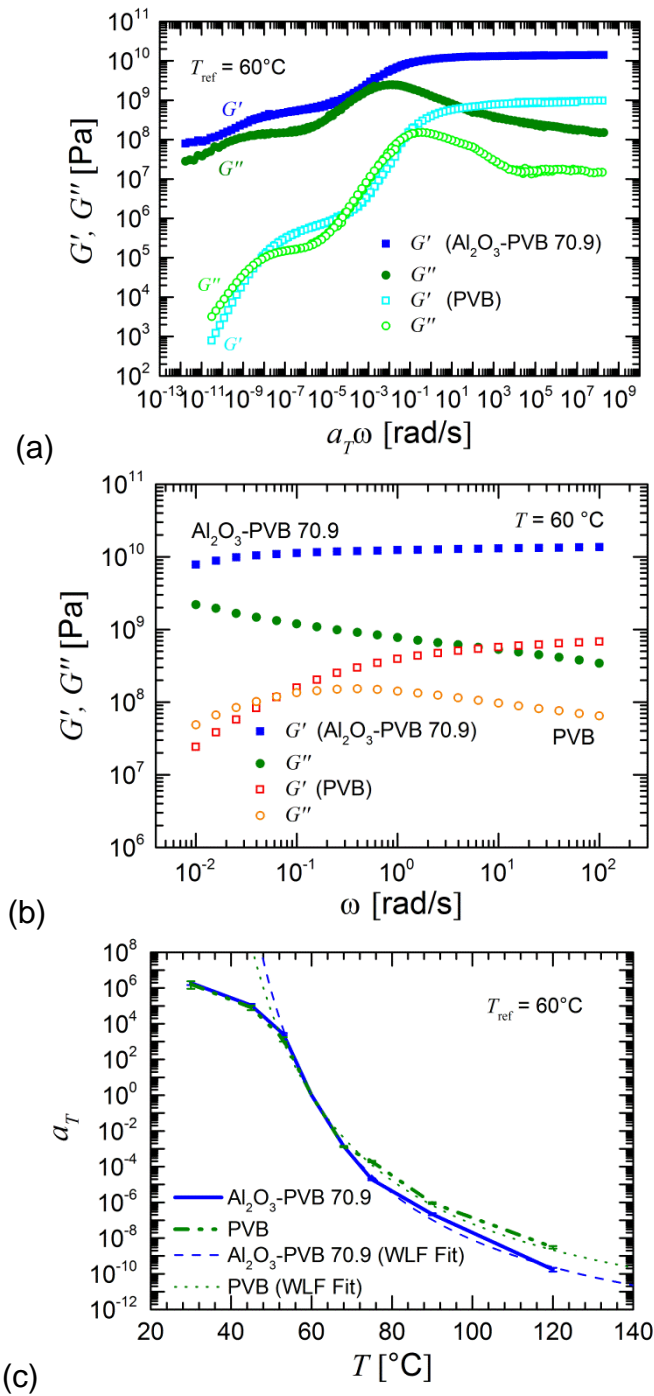
Figures 9(a) to (c)
 U.A. Handge et al.
 Polymer



Figures 10(a) and (b)

U.A. Handge et al.

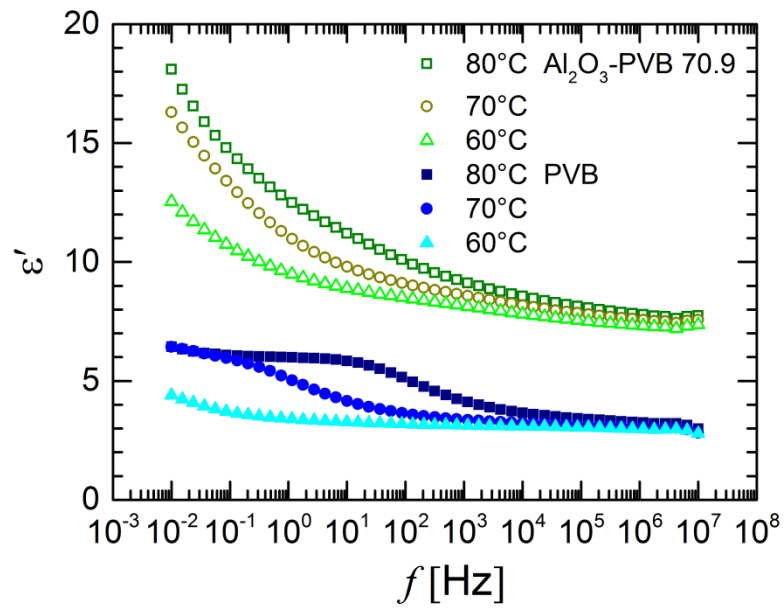
Polymer



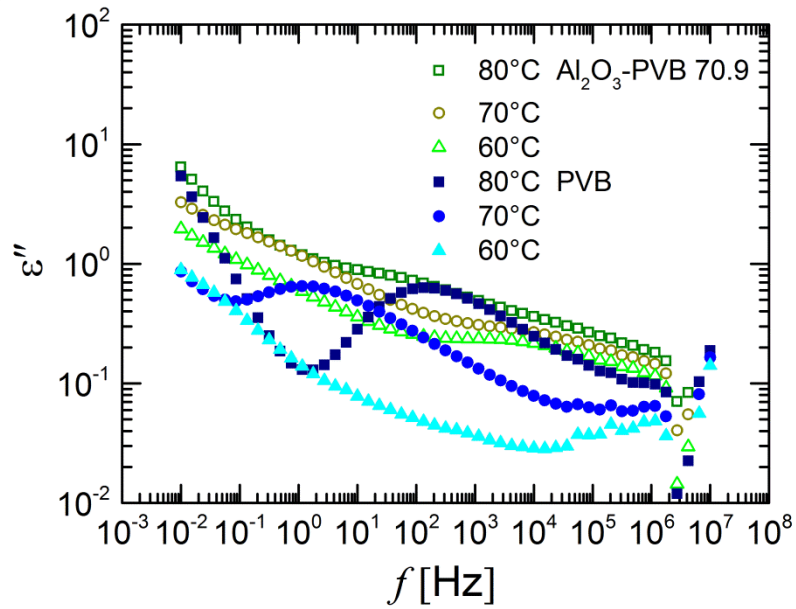
Figures 11(a) to (c)

U.A. Handge et al.

Polymer



(a)

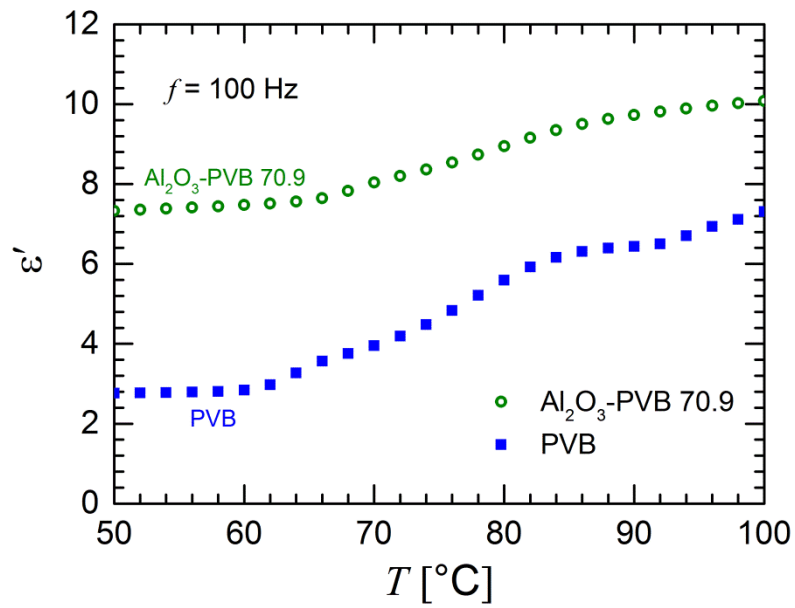


(b)

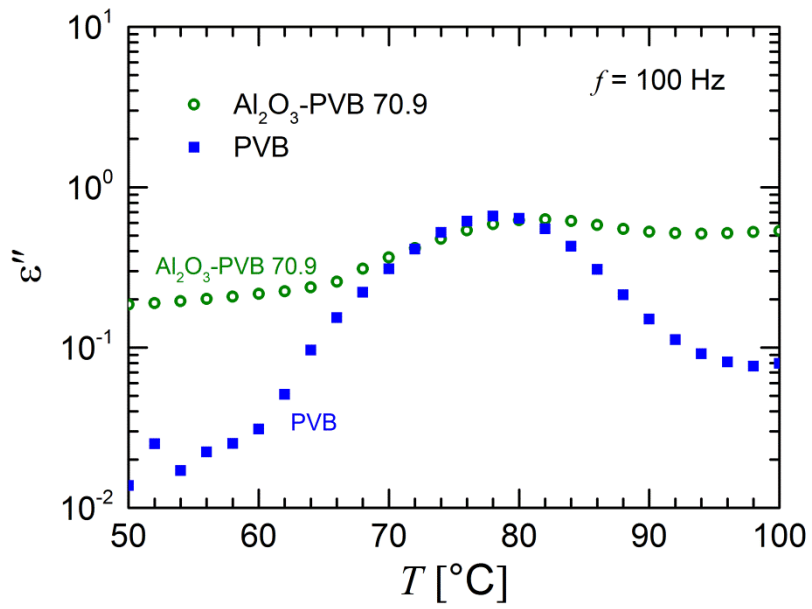
Figures 12(a) and (b)

U.A. Handge et al.

Polymer



(a)



(b)

Figures 13(a) and (b)

U.A. Handge et al.

Polymer